Solvothermal processes for nitride synthesis: examples of Li3GaN2 and graphitic C3N4 elaboration

Graziella Goglio, Annaïg Denis, Etienne Gaudin, Christine Labrugère, Denis Foy, Alain Largeteau

Solvothermal Processes for Nitride Synthesis: Examples of Li_3GaN_2 and Graphitic C_3N_4 Elaboration

Graziella Goglio, Annaïg Denis, Etienne Gaudin, Christine Labrugère, Denis Foy, and Alain Largeteau

Institut de Chimie de la Matière Condensée de Bordeaux-CNRS, Université Bordeaux 1, 87 avenue du Dr. A. Schweitzer, 33608 Pessac Cedex, France

Reprint requests to Dr. G. Goglio. Fax: (33)5400027 61. E-mail: goglio@icmcb-bordeaux.cnrs.fr

Z. Naturforsch. **2008**, *63b,* 730 – 738; received February 5, 2008

Dedicated to Professor Gérard Demazeau on the occasion of his 65th birthday

When precursors decompose or react in the presence of a solvent in a closed system at a temperature higher than the solvent's boiling point the reaction is called a solvothermal process. This reaction can be carried out either in supercritical or subcritical conditions, in homogeneous or heterogeneous systems, pressure and temperature being both key parameters. As the main interest of such processes is the enhancement of chemical reactivity, solvothermal reactions have been widely involved for nitride elaboration. We report two examples relative to solvothermal syntheses of nitrides. The first one deals with the elaboration of Li_3GaN_2: this ionic nitride has been successfully synthesized, structurally characterized and tested as nutrient for the ammonothermal GaN crystal growth. The second one is related to the elaboration of a well-crystallized graphitic carbon nitride (g-C_3N_4) aimed to be developed as a precursor for conversion towards dense CN_x phases.

Key words: Solvothermal Synthesis, Nitrides, Carbon Nitride, GaN, Li_3GaN_2

Introduction

Due to their wide technological applications, nitrides represent an important class of materials [1]. The use of high temperatures mainly imposed by the low chemical reactivity of the nitriding precursors (nitrogen gas or ammonia) does not favor the stabilization of metastable nitrides or the elaboration of nanocrystallites with homogeneous size and morphology. Then, during these last ten years, two different ways have been investigated for nitride synthesis: the high-pressure synthesis [2] and the solvothermal process [3].

A solvothermal reaction is defined as a reaction or a transformation of one or several precursors in the presence of a solvent in a close vessel at a temperature higher than the boiling point of the solvent [4]. This process allows the improvement of the chemical reactivity *via* an adequate choice of reagents and solvent. As a consequence, the pressure parameter is involved and can be autogeneous or not (in the first case it depends on the filling percentage of the vessel and the temperature, in the second one it depends on the starting pressure in the autoclave and the temperature). Moreover, depending on the nature of the chemical properties of the precursors and the solvent, the system can be either homogeneous or heterogeneous. Finally, the selected pressure and temperature conditions can imply subcritical or supercritical conditions for the system.

The nitriding sources originate either from the solvent or from the precursors. Then, three main nitriding solvents have been developped: ammonia (NH_3) [5], hydrazine (H_2NNH_2) [6] and 1,1,1,3,3,3-hexamethyldisilazane ($(CH_3)_3Si–NH–Si(CH_3)_3$) [7]. Concerning the precursors, two main nitriding chemical species have been investigated: N^{3-} mainly through the use of iono-covalent nitrides such as Li_3N, Mg_3N_2 [8, 9] or N_3^- choosing azides as precursors. In the last case NaN_3 has been widely used [10], nevertheless some other examples can be given such as $Ga(N_3)_3$ the decomposition of which leads to GaN [11].

To resume, solvothermal processes can be helpful either (i) to synthesize new nitrides, or (ii) for the elaboration of nanocrystallites well defined in size and morphology, or (iii) for crystal-growth processes. The elaboration of light element-based materials such as C_3N_4 [12] or cubic boron nitride [13] can be given as

an example for the first case. In the second case, regardless of the choice of reagents, solvents and nitriding species, suitable experimental pressure and temperature conditions must be chosen in order to control the mechanisms governing the nucleation and growth of nanocrystallites [14], the elaboration of InN nanocrystallites being an example [15]. Finally, in the third case, the ammonothermal crystal-growth process derived from the hydrothermal crystal-growth process of α-quartz [16] appears to be particularly suitable for elaboration of nitride crystals such as GaN [17].

Since 40 years, Professor Demazeau devoted a great part of his research activities to study the influence of high pressure on synthesis, shaping and physical properties of materials. Among his research topics, he widely investigated and developed solvothermal reactions either to synthetize new materials or to understand crystal-growth processes under high-pressure conditions. We describe here two different examples of solvothermal syntheses of nitrides which were initiated by Professor Demazeau and performed recently in his group with his fruitful and dynamic collaboration. The first one is related to the elaboration of Li_3GaN_2 which is proposed as a potential nutrient for GaN ammonothermal crystal growth. This solvothermal process leads to a powdered crystallized material which adopts a well-defined particle size. We show here the first GaN crystal-growth attempts with Li_3GaN_2 as nutrient. We finally present the solvothermal synthesis of a well-crystallized graphitic carbon nitride with a composition close to C_3N_4 and a significant hydrogen content.

Solvothermal Synthesis of a Potential Nutrient for Ammonothermal Crystal Growth of GaN

Wide band gap semiconductors such as gallium nitride (band gap = 3.4 eV) arouse considerable interest for many applications in short wavelength optoelectronics such as Light Emitting Diodes (LEDs), Laser Diodes (LDs), UV detectors and in microelectronics with high-power high-frequency transistors [18]. However, device development is nowadays limited because elaborated thin films exhibit a high density of defects due to the lack of suitable substrates. As a consequence, elaboration of GaN crystals has been a great challenge for two decades [19]. A recent survey on GaN crystal growth has evidenced that only few methods are relevant [17]. The HPNSG (High-Pressure-Nitrogen-Solution-Growth) process and the Na-flux crystal growth actually lead to the formation of the biggest crystals [20, 21]. The first one involves high nitrogen pressure (1 – 2 GPa) and high temperature (1400 – 1500 °C) using gallium as reagent, the second one is based on the use of gallium as reagent and Na flux (formed *in situ* by the decomposition of NaN_3 into Na and N_2) which acts as a catalyst for the dissociation of the N_2 molecules (in this case, pressure and temperature are lowered down to 5 – 10 MPa and 700 – 800 °C, respectively). Because these two processes both involve many difficulties for industrial developement, the ammonothermal route has also been recently investigated to elaborate GaN crystals in lower pressure and temperature conditions. First attempts leading to the formation of micrometric GaN crystallites were performed using supercritical ammonia as nitriding solvent, gallium metal as reagent and mineralizers such as an alkaline (lithium or potassium) amide or NH_4X (with X = halogen) [22, 23]. Finally, the ammonothermal synthesis of GaN has also been performed using amorphous GaN as nutrient, NH_3 as solvent and an amide or azide as mineralizer (attempts with a MNH_2 (with M = Na or K) mineralizer and a MX (with X = halogen) co-mineralizer were also successfully performed) [24, 25]. This last approach is based on the hydrothermal crystal-growth process of α-quartz.

Considering the great interest in the ammonothermal route to perform GaN crystal growth [26], we have chosen to adapt the process without using any mineralizer. This way, it was necessary to use a more ionic nutrient. By analogy with Li_3BN_2 used for cubic boron nitride solvothermal synthesis [27], we have focused our attention on Li_3GaN_2. Its synthesis and structural characterization are presented here. First attempts of the ammonothermal GaN crystal growth with Li_3GaN_2 as a nutrient are also described.

Experimental section

The reagents, lithium amide (Aldrich, 95 %) and gallium nitride (Aldrich, 99.99 %), were closely mixed and then introduced into an unclosed steel container, which was then placed into a high-pressure vessel (PER41, nickel alloy from Aubert et Duval). Until the vessel was closed, all steps were carried out in a glove box to prevent any oxidation or hydrolysis of the reagents. The high-pressure vessel was then filled with nitrogen (critical point: −146.9 °C, 3.4 MPa) and externally heated, the pressure increasing with temperature. The duration of the experiment was fixed to 6 h. Pressure and temperature were varied up to 150 MPa and 800 °C, respectively. The molar ratio Li_3N/GaN was taken equal to 1.2, the

Table 1. Atomic coordinates and atomic displacement parameters for Li_3GaN_2 (space group $Ia\bar{3}$).

Atom	Position	x	y	z	B_{iso} (Å^2)
N1	8*a*	0	0	0	0.3[a]
N2	24*d*	0.2273(3)	0	1/4	0.3[a]
Ga	16*c*	0.11769(12)	x	x	0.29(2)
Li	48*e*	0.1477(5)	0.3769(5)	0.111(2)	0.52(11)

[a] fixed value.

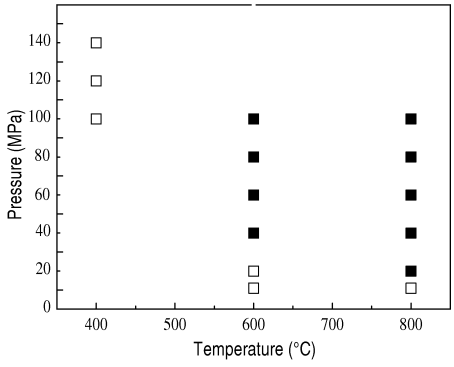

Fig. 1. Influence of the pressure and temperature conditions on the Li_3GaN_2 solvothermal synthesis (open square: no chemical reaction between reagents; full square: complete chemical reaction).

excess of lithium nitride being necessary to ensure a complete reaction as a small part of Li_3N is oxidized. After the synthesis, the powdered sample was protected from atmospheric moisture.

Scanning Electron Microscopy (SEM) has been carried out on the metallized (gold) powder with a JEOL JSM-6360A scanning electron microscope coupled with an Energy Dispersive X-ray Spectroscopy (EDXS) analyzer. Chemical elemental analysis was performed by ICP-AES (Inductive Coupled Plasma-Atomic Emission Spectroscopy) in the Service Central d'Analyse de Vernaison (CNRS, France).

Powder X-ray diffraction (XRD) data were collected at r. t. on a Philips PW1820 diffractometer (Bragg Brentano $\theta - 2\theta$ geometry) operating with Cu$K_{\alpha 1}$ and Cu$K_{\alpha 2}$ radiations over the angular range $5 \leq 2\theta \leq 110^\circ$ in steps of 0.02°. To avoid contact of the sample with air the powder was enclosed in a chamber filled with nitrogen with windows transparent for the X-ray beam (mylar foils). Structure refinement was carried out with the JANA2006 program package [28]. The background was simulated by Chebyshev polynoms and the peak shapes described by a pseudo-Voigt function with five profile coefficients. The refinement of peak asymmetry was performed using the Bérar-Baldinozzi function with two coefficients. The Li_2O impurity was considered in the refinement, and its amount was determined to be 6 weight-%. For Li_3GaN_2 the extinction conditions are in agreement with the cubic space group $Ia\bar{3}$. The unit-cell parameter is equal to 9.6149(3) Å. For the Rietveld refinement the atomic positions determined by Juza and Hund [29] were used as starting positions. Isotropic atomic displacement parameters (ADP) were refined for the Li1 and Ga1 positions and were fixed to 0.3 Å^2 for N1 and N2 nitrogen positions because of their negative value during the refinement. One can notice that the absolute value of the isotropic ADP of N1 and N2 and their standard uncertainties were of the same order of magnitude. The refinement converged to the reliability factors R_p = 7.18 %, R_{wp} = 10.59 % and R_B = 2.29 %. The final atomic positions are given in Table 1, the experimental and calculated powder pattern are displayed in Fig. 3.

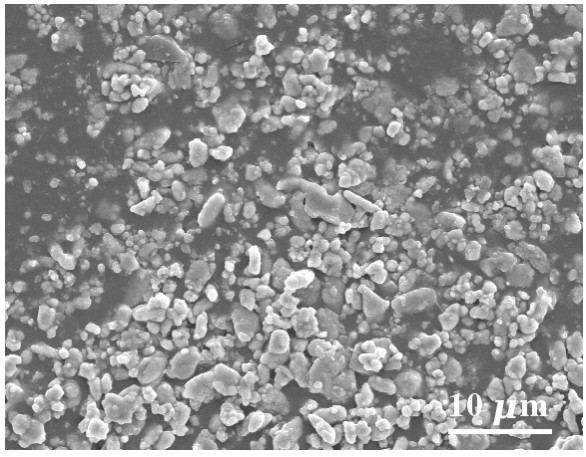

Fig. 2. Scanning electron microscopy image of Li_3GaN_2 synthetized at 90 MPa and 800 °C.

Further details of the crystal structure investigation may be obtained from Fachinformationszentrum Karlsruhe, 76344 Eggenstein-Leopoldshafen, Germany (fax: +49-7247-808-666; e-mail: crysdata@fiz-karlsruhe.de, http://www.fiz-informationsdienste.de/en/DB/icsd/depot_anforderung.html) on quoting the deposition number CSD-419137.

Ammonothermal crystal growth experiments for GaN were performed in a 100 mL high-pressure vessel. The Li_3GaN_2 nutrient was placed into an open gold tube at the bottom of the autoclave while a crystalline Si (1 0 0) substrate was hung up with a silver wire to the top of the vessel (these experiments were carried out in a glove box to prevent any oxidation or hydrolysis). The vessel was then filled with ammonia through a low-temperature condensation process (−35 °C) and heated in a three-zones furnace.

The deposit on the silicon substrate was characterized by X-ray photoelectron spectroscopy (XPS) on a ESCALAB 200i-XL XPS spectrometer equipped with a non-monochromatized MgK_α source. The analyzed area is about 250 μm in diameter. The pressure in the chamber was in the range of 10^{-7} Pa. The spectra have been fitted using the AVANTAGE program provided by Vacuum Generators.

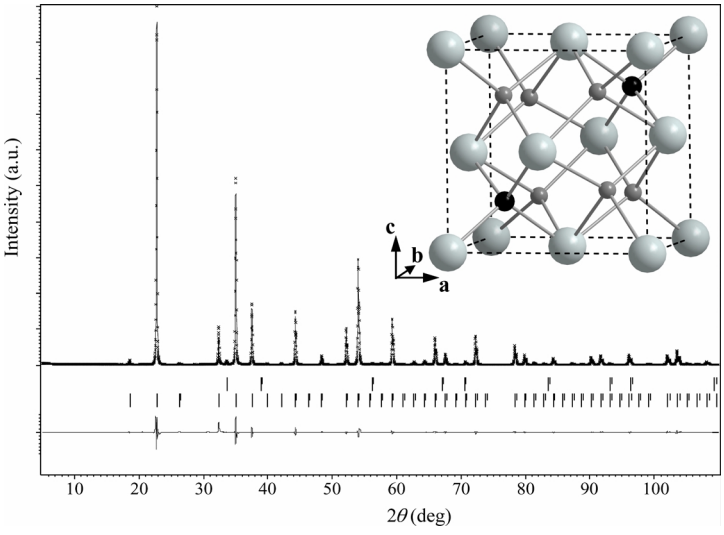

Fig. 3. Observed (cross), calculated (solid line), and difference (bottom) X-ray powder diffraction patterns for Li_3GaN_2 synthesized at 90 MPa and 800 °C. The tick marks indicate the reflection positions for Li_2O and Li_3GaN_2 (below). The inset shows the content of one-eighth of the unit cell. The large grey spheres correspond to the N^{3-} ions and the small grey and black spheres to Li^+ and Ga^{3+}, respectively.

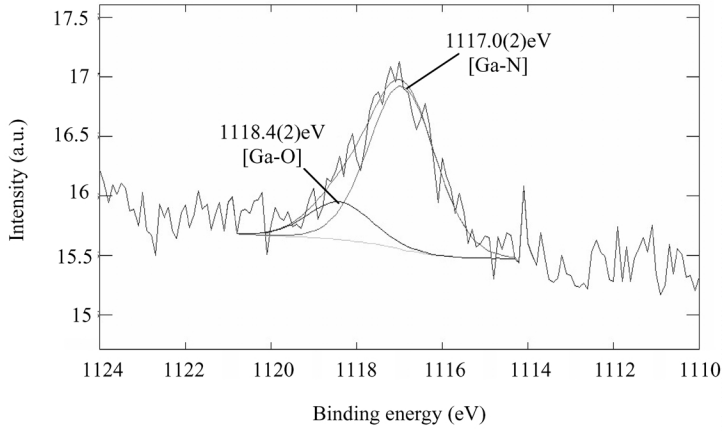

Fig. 4. Ga2$p_{3/2}$ spectrum of the deposit observed on the Si substrate, obtained in a transport experiment with Li_3GaN_2 as nutrient in subcritical ammonia.

Results and Discussion

The solvothermal process in supercritical nitrogen appears suitable to synthesize Li_3GaN_2 with a homogeneous grain size. Fig. 1 evidences that when the experimental temperature is lowered, pressure has to be increased to perform a complete reaction. We have then chosen 90 MPa and 800 °C for pressure and temperature conditions, respectively.

The resulting powder was off-white. The chemical analysis is consistent with the expected stoichiometry taking into account the presence of 6 weight-% Li_2O. The SEM micrograph presented in Fig. 2 evidences that the synthesized Li_3GaN_2 powder is constituted of grains quite homogeneous in size (1 – 4 μm). The EDXS analysis reveals a homogeneous Ga/N ratio from one Li_3GaN_2 grain to another, which tends to indicate a homogeneous chemical composition for the whole material. Li_3GaN_2 has first been synthesized by Juza and Hund [29]. Their process consisted in the treatment under a nitrogen flux at 400 °C of a Li_3Ga alloy. In this case, the grain size is widely inhomogeneous. These authors have also evidenced that Li_3GaN_2 could not be elaborated at atmospheric pressure with Li_3N and GaN as reagents which is consistent with our observations.

The structure of Li_3GaN_2 is derived from the antifluorite structure with a cubic close-packed array of nitrogen atoms and the tetrahedral sites filled by lithium and gallium atoms in an ordered way. The Li_3GaN_2 unit cell corresponds to eight times the antifluorite cell; one-eigth of this cell is shown in the inset of Fig. 3. Bond lengths and angle values indicate that the tetrahedral environment of the gallium atoms is regular while

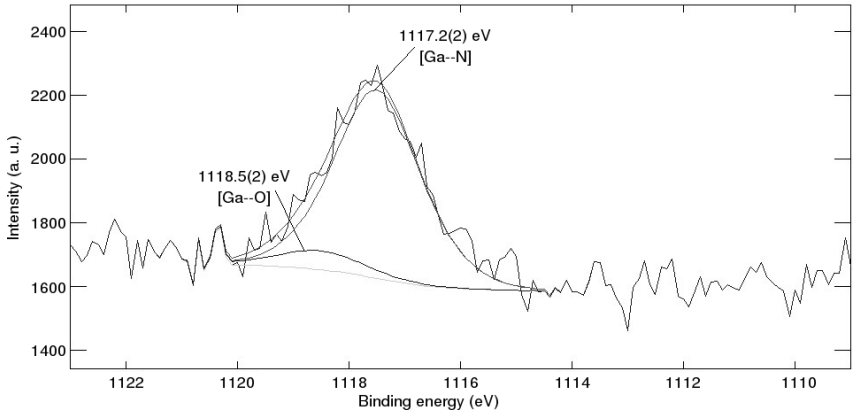

Fig. 5. Ga2$p_{3/2}$ spectrum of the deposit observed on the Si substrate, obtained in a transport experiment with Li_3GaN_2 as nutrient in supercritical ammonia.

the lithium atoms are in a quite distorted tetrahedral site. The gallium atoms form an infinite 3D network $[GaN_2]_8$ of corner sharing tetrahedra. The calculated bond valence (BV) sums are equal to 1.00(2), 2.657(6), 2.90(2), and 2.80(2) for Li, Ga, N1, and N2 positions, respectively. The values for the BV calculation are taken from Brese and O'Keefe [30]. These values confirm the proposed charge of $[GaN_2]^{3-}$ and indicate that the interaction between the $[GaN_2]^{3-}$ framework and the Li^+ ions is primarily ionic. As a consequence we strongly believe that Li_3GaN_2 could be a suitable nutrient for the ammonothermal crystal growth of gallium nitride without adding any mineralizer. We then expect the following mechanism:

(i) Li_3GaN_2 would firstly be dissociated in ammonia ($Li_3GaN_2 \rightarrow 3\ Li^+ + GaN_2^{3-}$), the ions being solvated by NH_3.

(ii) Because of the thermal gradient between the top and the bottom of the autoclave, the solvated "GaN_2^{3-}" species should be transported from the nutrient towards the substrate.

(iii) GaN should then be deposited on the substrate through the dissociation of "GaN_2^{3-}" anions ($GaN_2^{3-} \rightarrow GaN \downarrow + N^{3-}$).

We have then carried out some preliminary experiments to evaluate the feasibility of GaN ammonothermal crystal growth with Li_3GaN_2 as a nutrient. Attempts were performed either with subcritical (T = 117 °C, P = 150 MPa) or supercritical NH_3 (T = 144 °C, P = 200 MPa). In both cases, the thermal gradient ΔT between top ($T - \Delta T$) and bottom (T) of the autoclave was chosen equal to 10 °C to avoid flux turbulences. The duration of the experiment D was fixed to 48 h. Because D is short, the as-obtained deposits only consist of micrometric islands on the silicon substrate. They were characterized by XPS. In a preliminary study, Ga2$p_{3/2}$ spectra of metallic, oxidized and nitrided gallium were investigated, as references, Ga2$p_{3/2}$ was selected instead of Ga3d because it is totally separated from the oxygen lines [31]. A sample of gallium (with oxidized surface) and a GaN film were analyzed to determine the binding energy values for Ga–Ga, Ga–N and Ga–O. The obtained values were 1116.5(2), 1117.3(2) and 1118.5(2) eV, respectively.

Figs. 4 and 5 show the Ga2$p_{3/2}$ spectra of deposits obtained in subcritical and supercritical ammonia, respectively. In both cases, the signal can be resolved into two peaks the binding energies of which are characteristic of oxidized (1118.4(2) eV in Fig. 4 or 1118.5(2) eV in Fig. 5) and nitrided (1117.0(2) eV in Fig. 4 or 1117.2(2) eV in Fig. 5) gallium. The minor component has a contribution of $\sim 20\,\%$ and $\sim 10\,\%$ for experiments performed in subcritical and supercritical experiments, respectively. Moreover, the N/Ga molar ratio has also been estimated taking into account the integrated areas of the nitrogen component (N1s spectra are not presented here, the binding energies are consistent with N–Ga bonds) and the nitrided gallium component (Ga2$p_{3/2}$). The obtained values are 1.2 and 1.0 for subcritical and supercritical experiments, respectively. Thus, we can conclude that the deposit on the silicon substrate mainly consists of gallium nitride.

Conclusion

Li_3GaN_2 has been successfully synthesized by a solvothermal process. The as-obtained material is particularly homogeneous considering both its compo-

sition and the micrometric particle size. Some preliminary ammonothermal crystal-growth experiments were performed in order to determine the behavior of Li_3GaN_2 in supercritical ammonia. Since deposits mainly consisting of GaN were obtained, our results appear promising and tend to indicate that Li_3GaN_2 can be considered as a suitable nutrient.

Solvothermal Synthesis of a Well-crystallized Nitrogen-rich Graphitic Carbon Nitride

Light-element-based materials are of great interest owing to their specific physico-chemical properties (particularly hardness) mainly due to the strong covalency of the chemical bonds and to the three-dimensional character of the different structures they can adopt [32]. Liu and Cohen [33] first predicted that β-C_3N_4, an hypothetical carbon nitride similar in structure to β-Si_3N_4, may possess a bulk modulus of 427 GPa comparable to that of diamond. Further calculations have suggested other three-dimensional (3D) polymorphs, which are also expected to present low compressibility: α- and β-forms (isostructural to α-Si_3N_4 and β-Si_3N_4, respectively), a cubic form (derived from the high-pressure variety of Zn_2SiO_4) and a pseudocubic form (defective zinc-blende structure) [33 – 38]. Various graphitic (2D) forms were also suggested with either hexagonal or orthorhombic cells and different stackings of the graphene planes [38 – 40]. Until now many attempts have been made to synthesise these hypothetical carbon nitrides by means of various techniques either as bulk materials [12] or thin films [41]. Nevertheless they mainly lead to the formation of amorphous or poorly crystallized non-stoichiometric materials or to small crystallites embedded in an amorphous matrix.

The elaboration of C_3N_4 low-compressibility compounds can be direct or issued from a conversion process. In this latter case, processes developped in the case of diamond and cubic boron nitride synthesis could be performed [42]. These syntheses are based on a flux-assisted conversion process managed by the difference in solubility in an appropriate solvent of the low- and high-pressure forms. However, this process needs a low-density variety as precursor. Similar to the pure carbon system, it is expected that graphitic forms of C_3N_4 could be considered as adequate candidates. Consequently we have focused our attention on these layered materials.

Owing to the stability of the N_2 molecule easily formed when high temperatures are involved in the preparation process, it seems obvious to use low temperatures with precursors of high reactivity to synthesize graphitic C_3N_4. In this way a solvothermal process appears particularly interesting to enhance reactivity under mild thermal conditions.

Experimental section

Hydrazinium chloride (N_2H_5Cl) and carbon tetrachloride (CCl_4) were chosen as reagents with a molar ratio N_2H_5Cl/CCl_4 = 1/3. The mixture was introduced into a gold tube which was then sealed. To avoid the departure of volatile species, the bottom of the tube was placed into liquid nitrogen during welding. The sealed tube was then introduced into an autoclave. The vessel was filled with gaseous nitrogen which acted as pressure-transmitting medium. It was then placed into a tubular furnace and heated during 20 h at 500 °C and 100 MPa. After the synthesis, the as-obtained brown powder was washed with water, ethanol and acetone. The X-ray diffraction (XRD) pattern was obtained on a PANalytical X'Pert MPD X-ray diffractometer with CuK_α radiation. An infrared (IR) spectrum was recorded on an IR Paragon 1000 spectrophotometer. Bulk elemental combustion analysis of C, H, N elements was performed on a Thermofisher Flash EA 112 analyzer. Identification of chemical elements was carried out by EDXS in a Scanning Electron Microscope (SEM JEOL 6360A).

Results and discussion

CCl_4 has ever been chosen as carbon source in the presence of a nitriding reagent for the solvothermal synthesis of carbon nitride [43, 44]. Considering that the *in situ* formation of the nitriding species could enhance the nitriding power, hydrazinium chloride appeared as a suitable nitriding source because of its ability to decompose into NH_4Cl, N_2 and NH_3.

Fig. 6 shows the XRD pattern of the as-prepared powdered sample. The d values at 4.22, 3.52, 3.22, 2.56 and 1.60 Å can be assigned to the 100, 101, 002, 102 and 004 reflections, respectively. The corresponding parameters of the hexagonal cell are a = 4.87(2) and c = 6.41(2) Å. These values are in quite good agreement with those predicted by Teter and Hemley for hexagonal graphitic C_3N_4 and also match well with values reported by Bai *et al.* [44] for a graphitic carbon nitride obtained by an ammonothermal route. XRD characterization then revealed that the powder is a graphite-like C_3N_4 with a high degree of crystallinity.

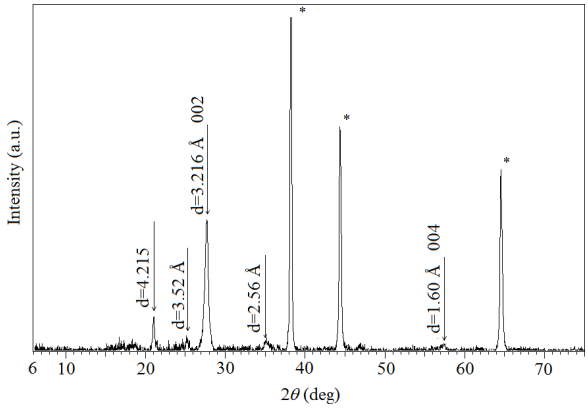

Fig. 6. X-Ray powder diffraction pattern of graphitic carbon nitride elaborated at 500 °C and 100 MPa. Asterisked peaks are attributed to gold particles originating from the sealed tube.

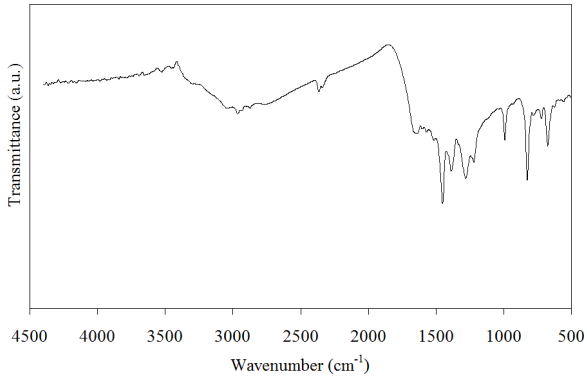

Fig. 7. Infrared spectrum of graphitic carbon nitride elaborated at 500 °C and 100 MPa. Carbon nitride powder was mixed with KBr and ground thoroughly, then pressed into pellets for characterization.

Bulk elemental combustion analysis (C, H, N elements) led to 0.71 – 0.75 and 1.06 – 1.15 molar ratios for C/N and C/H, respectively. The as-obtained composition $C_3N_{4.00-4.22}H_{2.60-2.83}$ reveals a stoichiometry in carbon and nitrogen which is close to the theoretical one for C_3N_4. In this case the solvothermal process thus has allowed the enhancement of the chemical reactivity, which ensures a high nitrogen content in the material.

The SEM characterization coupled with EDXS indicates that the grains have a micrometric size ($\sim$ 100 – 150 μm) and also contain traces of chlorine (5 %) and oxygen (0.2 %), the C/N molar ratio being estimated here to 0.6. Gold is also detected in the sample because some micrometric turnings are taken out from the metallic tube when the powder is extracted after the experiment. The IR spectrum is presented in Fig. 7. The major absorptions occur in the 1000 – 1650 cm^{-1} region, the sharp peaks being consistent with the stretching vibrations related to carbon/nitrogen single and double bonds. One should notice the absence of carbon/nitrogen triple-bond vibrations (no absorption at 2100 – 2200 cm^{-1}). The absorption at 820 cm^{-1} is characteristic for *s*-triazine ring vibrations (out-of-plane bending modes) suggesting that the (C_3N_3) motif is present in the graphene planes of the carbon nitride. The absorption band near 3000 cm^{-1} can probably originate from C–H rather than N–H bonds, which is quite uncommon in bulk carbon nitrides [12]. Finally the absorption peak at 670 cm^{-1} is consistent with the presence of C–Cl bonds in the material.

Cao *et al.* used NH_3 both as solvent and nitriding species in the presence of ferrous rods as catalyst (300 – 500 °C, 200 MPa) and CCl_4 as carbon source [43]. The presence of NH_4Cl as an impurity ensures the nitridation reaction. The as-obtained material is amorphous, the maximum molar nitrogen content being only 30 %. Triple bonds between carbon and nitrogen have been evidenced. When ammonia is replaced by NH_4Cl (which decomposes into HCl and NH_3) without any catalyst (reaction performed at 400 °C, with autogenous pressure), well-crystallized carbon nitride nanocrystals are obtained with a structure consistent with hexagonal graphitic C_3N_4 [44]. In this case single and double carbon/nitrogen bonds have been evidenced, as well as hydrogen/nitrogen bonds. In our case, similarly to Bai *et al.* [44], the *in situ* decomposition of hydrazinium chloride under solvothermal conditions tends to improve crystallinity and enhance the nitrogen content of the material.

Conclusion

Hydrazinium chloride has been shown to be a good nitriding agent using CCl_4 as carbon source. The *in situ* formation of nitriding species tends to enhance the nitriding power. The as-obtained material is particularly well-crystallized with a C/N molar ratio close to the theoretical one. Further characterizations will be needed (such as Nuclear Magnetic Resonance, Electron Energy Loss Spectroscopy, X-ray Photoelectron Spectroscopy) to confirm the way hydrogen and chlorine are bonded in the material. Moreover, conversion experiments will have to be attempted to evaluate the possible structural transitions of this graphitic carbon

nitride under pressure and temperature conditions towards dense phases.

Outlook

Solvothermal processes are a promising route for preparing nitrides. The new results can be especially important in four main domains in the near future:

(i) the stabilization of novel nitrides (in particular metastable compounds),

(ii) the elaboration of nanocrystallites with well defined size and morphology,

(iii) the crystal growth of functional nitrides in particular those involving industrial applications,

(iv) the development of new processes under mild pressure and temperature conditions, economically promising for developping nitrides with useful physico-chemical properties.

Acknowledgement

ISHA (International Solvothermal Hydrothermal Association) is acknowledged for its efforts for promoting solvothermal processes.

[1] J. E. Lowther, M. Amkreutz, T. Frauenheim, E. Kroke, R. Riedel, *Phys. Rev. B* **2003**, *68*, 0332011 – 0332014.
[2] E. Horvath-Bordon, R. Riedel, A. Zerr, P. F. Mc Millan, G. Auffermann, Y. Prots, W. Bronger, R. Kniep, P. Kroll, *Chem. Soc. Rev*. **2006**, *35*, 987 – 1014.
[3] G. Demazeau, G. Goglio, A. Denis, A. Largeteau, *J. Phys.: Condens. Matter* **2002**, *14*, 11085 – 11088.
[4] G. Demazeau, *J. Mater. Sci*., published online DOI 10.2007/s10853-007-2024-9.
[5] A. Wang, F. Capitain, V. Monnier, S. Matar, G. Demazeau, *J. Mat. Synth. Process*. **1997**, *5*, 235 – 248.
[6] H. Montigaud, B. Tanguy, G. Demazeau, I. Alves, S. Courjault, *J. Mater. Sci*. **2000**, *35*, 2547 – 2552.
[7] K. Sardar, C. N. R. Rao, *Solid State Sci*. **2005**, *7*, 217 – 220.
[8] Y. Xie, Y. Qian, W. Wang, S. Zhang, Y. Zhang, *Science* **1996**, *272*, 1926 – 1927.
[9] G. Zou, B. Hu, K. Xiong, H. Li, C. Dong, J. Liang, Y. Qian, *Appl. Phys. Lett*. **2005**, *86*, 1819011 – 1819013.
[10] P. Cai, Z. Yang, C. Wang, P. Xia, Y. Qian, *Mater. Lett*. **2006**, *60*, 410 – 413.
[11] L. Grocholl, J. Wang, E. G. Gillan, *Chem. Mater*. **2001**, *13*, 4290 – 4296.
[12] G. Goglio, D. Foy, G. Demazeau, *Mater. Sci. Eng. R* **2008**, *58*, 195 – 227.
[13] S. Dong, X. Hao, X. Xu, D. Cui, M. Jiang, *Mater. Lett*. **2004**, *58*, 2791 – 2794.
[14] G. Zou, H. Li, Y. Zang, K. Xiong, Y. Qian, *Nanotechnology* **2006**, *17*, S313–S320.
[15] J. Choi, E. G. Gillan, *J. Mater. Chem*. **2006**, *16*, 3774 – 3784.
[16] G. Demazeau, F. Lafon, J. Curtet, A. Largeteau, *High Press. Res*. **1994**, *12*, 329 – 335.
[17] A. Denis, G. Goglio, G. Demazeau, *Mater. Sci. Eng. R* **2006**, *50*, 167 – 194.
[18] J. Y. Duboz, *C. R. Acad. Sci. Série IV* **2000**, *1*, 71 – 80.
[19] T. F. Kuech, S. Gu, R. Wate, L. Zhang, J. Sun, J. A. Dumesic, J. M. Redwing, *Mater. Res. Soc. Symp. Proc*. **2001**, *639*, G1.1.1–G1.1.11.
[20] I. Grzegory, J. Jun, S. Krukowski, M. Bockowski, S. Porowski, *Physica B* **1993**, *185*, 99 – 102.
[21] H. Yamane, M. Shimada, S. J. Clarke, F. J. DiSalvo, *Chem. Mater*. **1997**, *9*, 413 – 416.
[22] R. Dwilinski, R. Doradzinski, J. Garczynski, L. Sierzputowski, J. M. Baranowski, M. Kaminska, *Diamond Relat. Mater*. **1998**, *7*, 1348 – 1350.
[23] A. P. Purdy, *Chem. Mater*. **1999**, *11*, 1648 – 1651.
[24] D. R. Ketchum, J. W. Kolis, *J. Cryst. Growth* **2001**, *222*, 431 – 434.
[25] B. Raghothamachar, W. M. Vetter, M. Dudley, R. Dalmau, R. Schelesser, Z. Sitar, E. Michaels, J. W. Kolis, *J. Cryst. Growth* **2002**, *246*, 271 – 280.
[26] T. Fukuda, D. Ehrentraut, *J. Crystal Growth* **2007**, *305*, 304 – 310.
[27] G. Demazeau, V. Gonnet, V. Solozhenko, B. Tanguy, H. Montigaud, *C. R. Acad. Sci. Série IIB* **1995**, *320*, 419 – 422.
[28] V. Petříček, M. Dušek, L. Palatinus, JANA2006, The Crystallographic Computing System, Institute of Physics, Praha (Czech Republic) **2006**.
[29] R. Juza, F. Hund, *Z. Anorg. Allg. Chem*. **1948**, *257*, 13 – 25.
[30] N. E. Brese, M. O'Keefe, *Acta Crystallogr*. **1991**, *B47*, 192 – 197.
[31] D. Briggs, M. P. Seah (Eds.), *Practical Surface Analysis*, Vol. 1 (2nd ed.), John Wiley, Chichester **1990**.
[32] R. Riedel, *Adv. Mater*. **1994**, *6*, 549 – 560.
[33] A. Y. Liu, M. L. Cohen, *Science* **1989**, *245*, 841 – 842.
[34] A. Y. Liu, M. L. Cohen, *Phys. Rev. B* **1990**, *41*, 10727 – 10734.
[35] A. Y. Liu, R. M. Wentzcovitch, *Phys. Rev. B* **1994**, *50*, 10362 – 10365.
[36] Y. Guo, W. A. Goddard, *Chem. Phys. Lett*. **1995**, *237*, 72 – 76.
[37] J. Martin-Gil, F. J. Martin-Gil, M. Sarikaya, M. Qian, M. José-Yacaman, *J. Appl. Phys*. **1997**, *81*, 2555 – 2559.
[38] D. M. Teter, R. J. Hemley, *Science* **1996**, *271*, 53 – 55.

[39] I. Alves, G. Demazeau, B. Tanguy, F. Weill, *Solid State Commun*. **1999**, *109*, 697 – 701.
[40] Z. Zhang, H. Guo, G. Zhong, F. Yu, Q. Xiong, X. Fan, *Thin Solid Films* **1999**, *346*, 96 – 99.
[41] S. Muhl, J. M. Mendez, *Diamond. Relat. Mater*. **1999**, *8*, 1809 – 1830.
[42] L. Vel, G. Demazeau, J. Etourneau, *Mater. Sci. Eng. B* **1991**, *10*, 149 – 164.
[43] Y. G. Cao, X. L. Chen, Y. C. Lan, J. Y. Li, Y. P. Xu, T. Xu, *Appl. Phys. A* **2000**, *71*, 465 – 467.
[44] Y. J. Bai, B. Lu, Z. G. Liu, L. Li, D. L. Cui, X. G. Xu, Q. L. Wang, *J. Cryst. Growth* **2003**, *247*, 505 – 508.